

Parameterization of Manifold Triangulations

Michael S. Floater, Kai Hormann, Martin Reimers

Abstract. This paper proposes a straightforward method of parameterizing manifold triangulations where the parameter domain is a coarser triangulation of the same topology. The method partitions the given triangulation into triangular patches bounded by geodesic curves and parameterizes each patch individually. We apply the global parameterization to remeshing and wavelet decomposition.

§1. Introduction

This paper deals with the parameterization of manifold triangulations of arbitrary topology. By a triangle T we mean the convex hull of three non-collinear points $v_1, v_2, v_3 \in \mathbb{R}^3$, *i.e.*, $T = [v_1, v_2, v_3]$. We call a set of triangles $\mathcal{T} = \{T_1, \dots, T_m\}$ a manifold triangulation if

- 1) $T_i \cap T_j$ is either empty, a common vertex, or a common edge, $i \neq j$, and
- 2) $\Omega_{\mathcal{T}} = \bigcup_{i=1}^m T_i$ is an orientable 2-manifold.

In this paper we propose a method for constructing a parameterization of a given manifold triangulation \mathcal{T} over a coarse manifold triangulation \mathcal{D} . By parameterization, we mean a homeomorphism,

$$\phi : \Omega_{\mathcal{D}} \rightarrow \Omega_{\mathcal{T}},$$

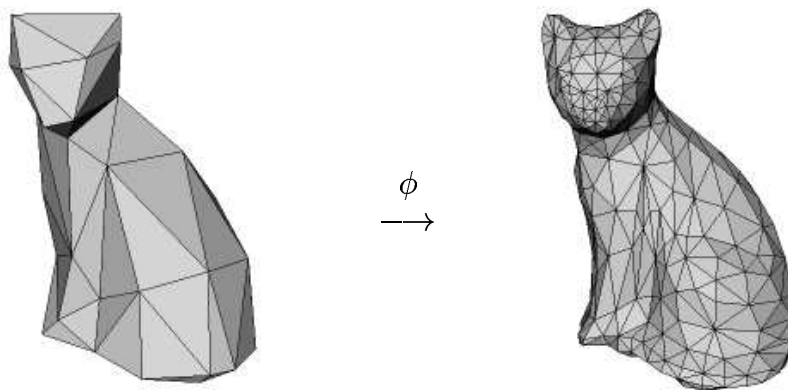


Fig. 1. Parameterization.

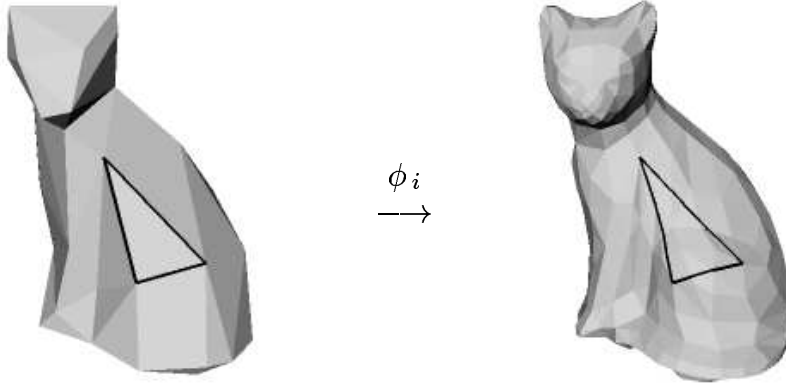


Fig. 2. Local parameterization.

as illustrated in Fig. 1. Thus $\Omega_{\mathcal{D}}$ will be the parameter domain of $\Omega_{\mathcal{T}}$ and ϕ will be bijective, continuous, and have a continuous inverse.

The basic idea is to partition $\Omega_{\mathcal{T}}$ into triangular surface patches S_i , each bounded by geodesic curves, such that there is a one-to-one correspondence between the triangles T_i of \mathcal{D} and the patches S_i . We then construct local, piecewise linear parameterizations

$$\phi_i : T_i \rightarrow S_i,$$

as illustrated in Fig. 2, which match pairwise at the vertices and edges of \mathcal{D} so that the combined mapping

$$\phi(x) = \phi_i(x), \quad x \in T_i,$$

is also continuous and one-to-one.

The first method for parameterizing manifold triangulations was that of Eck et al. [5], who proposed partitioning by growing Voronoi-like regions. Local parameterization was done through discrete harmonic maps. Later, Lee et al. [16] proposed a method in which the parameterization is carried out iteratively in parallel with mesh simplification. We believe our method is conceptually simpler and unlike in [5] and [16], it guarantees a one-to-one parameterization under only mild conditions on the parameter domain.

We complete the paper by giving an application of the method to a wavelet decomposition of the surface $\Omega_{\mathcal{T}}$. We subdivide the parameter domain dyadically and sample the surface $\Omega_{\mathcal{T}}$ at the vertices, yielding an approximate surface $\Omega_{\mathcal{S}}$ which can be decomposed using some chosen wavelet scheme.

After completing this paper, we became aware of the recent publication [21] where geodesic curves are also used to partition the triangulation.

§2. Finding the Parameter Domain

Before we construct a parameterization, we need to determine an appropriate parameter domain, which in this setting will be a manifold triangulation \mathcal{D}

of the same topology as \mathcal{T} , but with typically much fewer triangles. Thus we regard \mathcal{T} as a fine triangulation and \mathcal{D} as a coarse one. Moreover, for our method, we also need a correspondence between the vertices of \mathcal{D} and some suitable points on $\Omega_{\mathcal{T}}$. We will make clear what we mean by ‘suitable’ later.

If we are not given a parameter domain and correspondence in advance, we propose using one of the many known algorithms for *mesh decimation* to find one. For a survey of methods, see [11,15]. One major class of these algorithms modifies a given triangulation by iteratively applying a decimation operator such as *vertex removal* or *half-edge collapse* that decreases the number of triangles by two in each step without changing the topology of the mesh surface. All these algorithms result in a coarser triangulation \mathcal{D} that approximates the shape of the initial mesh \mathcal{T} . Moreover, these algorithms usually provide a correspondence between the vertices v_i of \mathcal{D} and points on $\Omega_{\mathcal{T}}$. In fact, many of these algorithms never move vertices at each step, only delete them, in which case the vertices of the final coarse triangulation are also vertices of the original triangulation \mathcal{T} . In our numerical examples, we have used the method of Campagna [1].

§3. Partitioning

The first step in the parameterization method is to partition the surface $\Omega_{\mathcal{T}}$ into triangular regions S_i corresponding to the triangles T_i of \mathcal{D} .

Recall that for each vertex v_j of \mathcal{D} there is a suitable corresponding point x_j in $\Omega_{\mathcal{T}}$. Then for each edge $[v_j, v_k]$ of \mathcal{D} we construct a shortest geodesic path $\Gamma(x_j, x_k) \subset \Omega_{\mathcal{T}}$ between the two points x_j and x_k of $\Omega_{\mathcal{T}}$. We suppose that the parameter domain and vertex correspondence are such that these geodesic paths partition the surface $\Omega_{\mathcal{T}}$ into triangular patches corresponding to the triangles of \mathcal{D} . Thus to each triangle $T_i = [v_j, v_k, v_\ell]$ there should be a triangular region $S_i \subset \Omega_{\mathcal{T}}$ bounded by the three curves $\Gamma(x_j, x_k)$, $\Gamma(x_k, x_\ell)$, $\Gamma(x_\ell, x_j)$. In this case the patches $\{S_i\}$ constitute a surface triangulation of the surface $\Omega_{\mathcal{T}}$ corresponding to the triangulation \mathcal{D} . In fact, it is known in graph theory [10], that the curves will induce such a surface triangulation if

- 1) the only intersections between the curves is at common endpoints and
- 2) the cyclic ordering of the curves around a common vertex is the same as the cyclic ordering of the corresponding edges in \mathcal{D} .

We thus require a parameter domain $\Omega_{\mathcal{D}}$ and a vertex correspondence with the property that conditions (1) and (2) hold. We have found in our numerical examples that these conditions have always been met, where we have used mesh decimation to generate \mathcal{D} , under one of the usual stopping criteria. In fact, theoretically we could ensure that conditions (1) and (2) hold, by simply making them part of the stopping criterion. In practice, however, we did not find this necessary.

Since the shortest path across a triangle is a straight line we see that geodesics on triangulations are polygonal curves with nodes lying on the edges of the triangulation. Thus a minimal geodesic corresponding to the edge

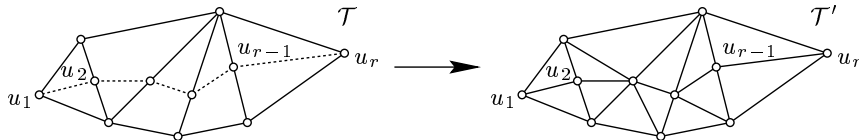


Fig. 3. Refining \mathcal{T} in order to embed a geodesic curve.

$[v_j, v_k]$ of \mathcal{D} is a union of line segments,

$$\Gamma(x_j, x_k) = [u_1, u_2] \cup [u_2, u_3] \cup \cdots \cup [u_{r-1}, u_r], \quad (1)$$

where $u_1 = x_j$, $u_r = x_k$, and the points u_p are located on the edges of \mathcal{T} . We can therefore insert all segments of these geodesics curves into the triangulation \mathcal{T} , yielding a refined triangulation \mathcal{T}' . All points u_p will become vertices in \mathcal{T}' and the segments $[u_p, u_{p+1}]$ will become edges of \mathcal{T}' . The geometry of \mathcal{T}' is the same as that of \mathcal{T} , *i.e.*, $\Omega_{\mathcal{T}'} = \Omega_{\mathcal{T}}$. Fig. 3 illustrates the refinement when the endpoints x_j and x_k of the curve are themselves vertices of \mathcal{T} , which is the case in our implementation. In this case, each segment $[u_p, u_{p+1}]$ will split the triangle in \mathcal{T} containing it into one triangle and one quadrilateral. When making the refinement \mathcal{T}' , we simply split the quadrilateral into two triangles by choosing either one of the two diagonals.

If one of the points x_j was not a vertex of \mathcal{T} , we would apply a pre-process before applying the above procedure. In the pre-process, we would insert x_j into \mathcal{T} by adding appropriate edges emanating from it, depending on whether x_j lies on an edge of \mathcal{T} or is in the interior of some triangle of \mathcal{T} ; see Fig. 4.

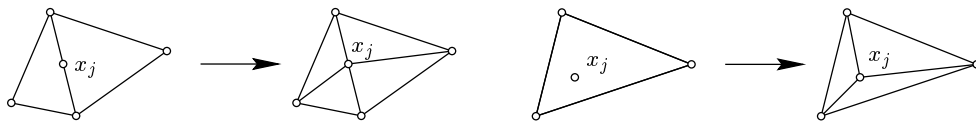


Fig. 4. Pre-process of inserting a point x_j into \mathcal{T} .

The problem of computing geodesics on polygonal surfaces is a classic one and has received considerable attention, see *e.g.* [2,12,14,17,18]. We have used Chen and Han's shortest path algorithm [2]; see also [12]. The method is exact and based on unfolding triangles. However, as the method is computationally quite expensive, we compute the geodesic $\Gamma(x_j, x_k)$ by restricting the search to a small subtriangulation \mathcal{T}_{jk} of \mathcal{T} . The shape of \mathcal{T}_{jk} is chosen to be an 'ellipse' with x_j and x_k its 'focal points'. We take \mathcal{T}_{jk} to be the set of all triangles in \mathcal{T} containing a vertex v of \mathcal{T} such that

$$d_a(v, x_j) + d_a(v, x_k) \leq K d_a(x_j, x_k),$$

where $d_a(x, y)$ denotes an *approximation* to the geodesic distance $d(x, y)$ between two points x and y of $\Omega_{\mathcal{T}}$, and $K > 1$ is some chosen constant. The idea here is that we can use a much faster algorithm to compute the approximative

distance $d_a(x, y)$. We have used the method of Kimmel and Sethian [14] to compute $d_a(x, y)$ and subsequently find \mathcal{T}_{jk} . Since the latter method gives such a close approximation to the true geodesic distance, we have been able to set $K = 1.06$ and then in almost all cases we have run, the geodesic path $\Gamma(x_j, x_k)$ has been contained in $\Omega_{\mathcal{T}_{jk}}$. In the event that the path is not contained in $\Omega_{\mathcal{T}_{jk}}$, we simply increase K . Eventually, for large enough K we are guaranteed to locate $\Gamma(x_j, x_k)$.

The point about the refinement is that each patch $S_i \subset \Omega_{\mathcal{T}}$ is now the union of triangles in \mathcal{T}' , *i.e.*,

$$S_i = \Omega_{\mathcal{T}_i},$$

where \mathcal{T}_i is a subtriangulation of \mathcal{T}' . This will enable us to apply a standard parameterization method to parameterize each patch S_i .

§4. Parameterization

For each triangle $T_i = [v_j, v_k, v_\ell]$ of \mathcal{D} we now have a corresponding triangular patch $S_i \subset \Omega_{\mathcal{T}}$, the union of the triangles in a subtriangulation \mathcal{T}_i of \mathcal{T}' . It remains to construct a parameterization $\phi_i : T_i \rightarrow S_i$. We do this by taking ϕ_i to be the inverse of a piecewise linear mapping $\psi_i : S_i \rightarrow T_i$. In other words ψ_i will be continuous over S_i and linear over each triangle in \mathcal{T}_i . By linear (or affine), we mean that for any triangle $T = [v_1, v_2, v_3]$ in \mathcal{T}_i ,

$$\psi_i(\lambda_1 v_1 + \lambda_2 v_2 + \lambda_3 v_3) = \lambda_1 \psi_i(v_1) + \lambda_2 \psi_i(v_2) + \lambda_3 \psi_i(v_3), \quad (2)$$

for any real numbers $\lambda_1, \lambda_2, \lambda_3 \geq 0$ which sum to one. Thus ψ_i will be completely determined by the parameter points $\psi_i(v) \in \mathbb{R}^3$ for vertices v of \mathcal{T}_i .

We will use the method of [6]. First of all, due to construction, corresponding to the vertices v_j, v_k, v_ℓ of T_i , there must be three corresponding ‘corner’ vertices x_j, x_k, x_ℓ in the boundary of \mathcal{T}_i . We therefore set $\psi_i(x_r) = v_r$, for $r \in \{j, k, \ell\}$. Next we determine ψ_i at the remaining boundary vertices of \mathcal{T}_i . The boundary of \mathcal{T}_i consists of three geodesic curves, each with endpoints in $\{x_j, x_k, x_\ell\}$. Consider the edge $[v_j, v_k]$ and the corresponding geodesic curve $\Gamma(x_j, x_k)$ in (1). We take ψ_i at the vertices u_p to be a chord length parameterization, that is we demand that

$$\psi_i(u_p) = (1 - \lambda_p) \psi_i(u_1) + \lambda_p \psi_i(u_r),$$

where

$$\lambda_p = \frac{L_p}{L_r} \quad \text{with} \quad L_p = \sum_{q=1}^{p-1} \|u_{q+1} - u_q\|,$$

Finally, we determine ψ_i at the interior vertices of \mathcal{T}_i by solving a sparse linear system of equations. For each interior vertex v of \mathcal{T}_i , we demand that

$$\psi_i(v) = \sum_{w \in N_v} \lambda_{vw} \psi_i(w),$$

where the weights λ_{vw} are strictly positive and sum to one. Here N_v denotes the set of neighbouring vertices of v . It was shown in [6] that this linear system always has a unique solution. We take the weights λ_{vw} to be the shape-preserving weights of [6], which were shown to have a reproduction property and tend to minimize distortion.

Since the equations force each point $\psi_i(v)$ to be a convex combination of its neighbouring points $\psi_i(w)$, ψ_i is a so-called convex combination map. As to the question of whether ψ_i is injective, we have the following.

Proposition 1. *The mapping $\psi_i : S_i \rightarrow T_i$ is one-to-one.*

Proof: Due to Theorem 6.1 of [7], it is sufficient to show that no dividing edge of T_i is mapped into the boundary of T_i . By a dividing edge we understand an edge $[v, w]$ of T_i which is an interior edge of T_i and whose endpoints v and w are boundary vertices of T_i . Thus we simply need to show that for such an edge, the two mapped points $\psi_i(v)$ and $\psi_i(w)$ do not belong to the same edge of T_i .

Assume for the sake of contradiction that the points $\psi_i(v)$ and $\psi_i(w)$ belong to the same edge of T_i . Due to our construction this implies that v and w lie on the same geodesic curve. Since the edge $[v, w]$ is obviously the shortest geodesic curve connecting v and w it must belong to the boundary of T_i , contradicting our assumption that $[v, w]$ is a dividing edge. \square

We complete this section by showing that the method has linear precision in the sense that the parameterization ϕ is locally linear if $\Omega_{\mathcal{T}}$ is locally planar.

Proposition 2. *Suppose that for some triangle $T_i = [v_j, v_k, v_\ell]$, the triangle $[x_j, x_k, x_\ell]$ is contained in $\Omega_{\mathcal{T}}$. Then we have $S_i = [x_j, x_k, x_\ell]$ and the mapping $\phi_i : T_i \rightarrow S_i$ is linear in the sense of (2).*

Proof: If $[x_j, x_k, x_\ell] \subset \Omega_{\mathcal{T}}$, then the line segments $[x_j, x_k]$, $[x_k, x_\ell]$, $[x_\ell, x_j]$ are the geodesic boundary curves of S_i since they are trivially shortest paths, and thus $S_i = [x_j, x_k, x_\ell]$. Due to chord length parameterization of the boundary curves, the whole boundary of S_i is mapped affinely into the boundary of T_i . Since moreover we use shape-preserving parameterization for interior vertices, Proposition 6 in [6] shows that ψ_i , and therefore ϕ_i , is linear. \square

In fact, due to construction, the whole parameterization ϕ depends continuously on the vertices of \mathcal{T} . This implies that when $\Omega_{\mathcal{T}}$ is locally close to being planar, the parameterization ϕ will locally be close to being linear.

§5. Application to Wavelet Decomposition

The parameterization ϕ of the manifold surface $\Omega_{\mathcal{T}}$ allows us to approximate $\Omega_{\mathcal{T}}$ by a new manifold surface which can be decomposed using a wavelet scheme.

To explain how this works, first set $\mathcal{D}^0 = \mathcal{D}$ and consider its dyadic refinement \mathcal{D}^1 . By dyadic refinement we mean that we divide each triangle $T = [v_1, v_2, v_3]$ in \mathcal{D}^0 into the four congruent subtriangles,

$$[v_1, w_2, w_3], \quad [w_1, v_2, w_3], \quad [w_1, w_2, v_3], \quad [w_1, w_2, w_3],$$

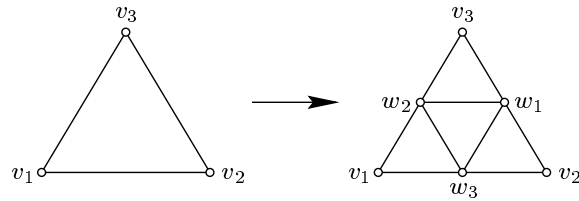


Fig. 5. Dyadic refinement.

where

$$w_1 = \frac{v_2 + v_3}{2}, \quad w_2 = \frac{v_3 + v_1}{2}, \quad w_3 = \frac{v_1 + v_2}{2},$$

are the midpoints of the edges of T ; see Fig. 5. This refinement is also referred to as the one-to-four split, and the set of all such subtriangles forms a triangulation \mathcal{D}^1 . Similarly, we can refine \mathcal{D}^1 to form \mathcal{D}^2 , and so on and we have $\Omega_{\mathcal{D}_j} = \Omega_{\mathcal{D}}$ for all $j = 0, 1, \dots$

Next let S^j be the linear space of all functions $f^j : \Omega_{\mathcal{D}} \rightarrow \mathbb{R}^3$ which are continuous on $\Omega_{\mathcal{D}}$ and linear on each triangle of \mathcal{D}^j . These linear spaces are clearly nested,

$$S^0 \subset S^1 \subset S^2 \subset \dots,$$

and the dimension of S^j is the number of vertices in \mathcal{D}^j .

The nested spaces S^j allow us to set up a multiresolution framework which can be used to decompose a given element f^j of S^j . For each $j = 1, 2, \dots$, we choose W^{j-1} to be some subspace of S^j such that

$$S^{j-1} \oplus W^{j-1} = S^j,$$

where \oplus denotes in general a direct sum. We call W^{j-1} a *wavelet space* and we can decompose any space S^j into its coarsest subspace S^0 and a sequence of wavelet spaces,

$$S^j = S^{j-1} \oplus W^{j-1} = \dots = S^0 \oplus W^0 \oplus \dots \oplus W^{j-1}. \quad (3)$$

Within this framework, we can decompose a given function $f^j \in S^j$ into *levels of detail*. Equation (3) implies that there exist unique functions $f^{j-1} \in S^{j-1}$ and $g^{j-1} \in W^{j-1}$ such that

$$f^j = f^{j-1} + g^{j-1},$$

and we regard f^{j-1} as an approximation to f^j at a lower resolution or level of detail. The function g^{j-1} is the error introduced when replacing the original function f^j by its approximation f^{j-1} . We can continue this decomposition until $j = 0$. Then we will have $f^0 \in S^0$ and $g^i \in W^i$, $i = 0, 1, \dots, j - 1$ with

$$f^j = f^0 + g^0 + g^1 + \dots + g^{j-1},$$

and f^0 will be the coarsest possible approximation to f^j .

Now, we can use the parameterization $\phi : \Omega_{\mathcal{D}} \rightarrow \Omega_{\mathcal{T}}$ to decompose and approximate $\Omega_{\mathcal{T}}$. We simply let f^j be that element of S^j such that

$$f^j(v) = \phi(v),$$

for all vertices v of \mathcal{D}^j . For sufficiently large j , f^j will be a good approximation to ϕ in which case the Hausdorff distance between $\Omega_{\mathcal{T}}$ and the image $f^j(\Omega_{\mathcal{D}})$ will be small. Thus a wavelet decomposition of f^j will be an approximate decomposition of ϕ and hence the manifold $\Omega_{\mathcal{T}}$ itself.

Many wavelet spaces and bases have been proposed for decomposing piecewise linear spaces over triangulations, see for example [8,22]. In our implementation we have taken the wavelet space W^{j-1} to be orthogonal to S^{j-1} with respect to the weighted inner product

$$\langle f, g \rangle = \sum_{T \in \mathcal{D}} \frac{1}{a(T)} \int_T f(x)g(x) dA, \quad f, g \in C(\Omega_{\mathcal{D}})$$

where $a(T)$ is the area of triangle T . For the wavelet basis we have applied the wavelets constructed in [8] which generalize to this manifold setting in a trivial way. As usual we used the hat (nodal) functions as bases for the nested spaces S^j themselves. We have implemented the filterbank algorithms developed in [9], adapted to this manifold setting.

§6. Numerical Example

Though the parameterization method applies to manifolds of arbitrary topology, we will simply illustrate with the manifold triangulation \mathcal{T} on the left of Fig. 6, which is homeomorphic to a sphere. We first computed a coarser triangulation \mathcal{D} by mesh decimation as described in [1], shown on the right of Fig. 6.

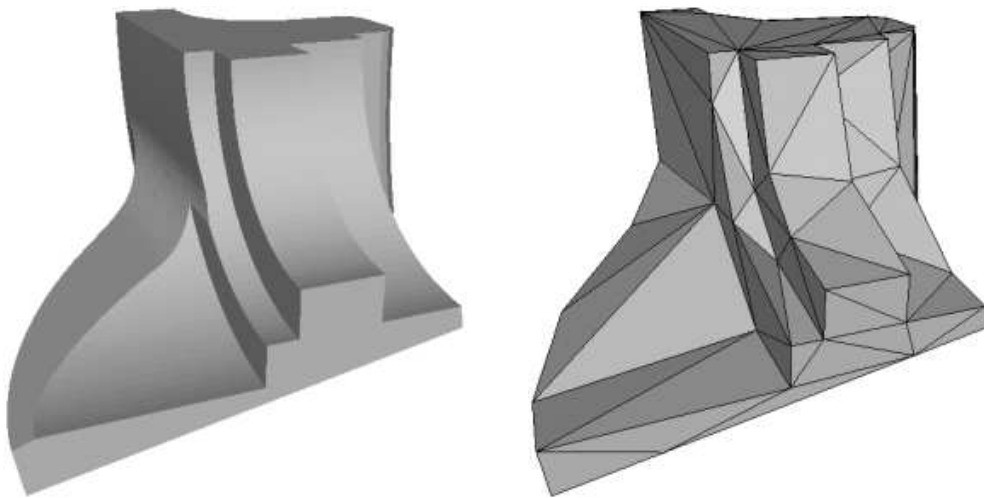


Fig. 6. Fine triangulation \mathcal{T} with 12,946 triangles (left) and coarse triangulation \mathcal{D} with 114 triangles (right).

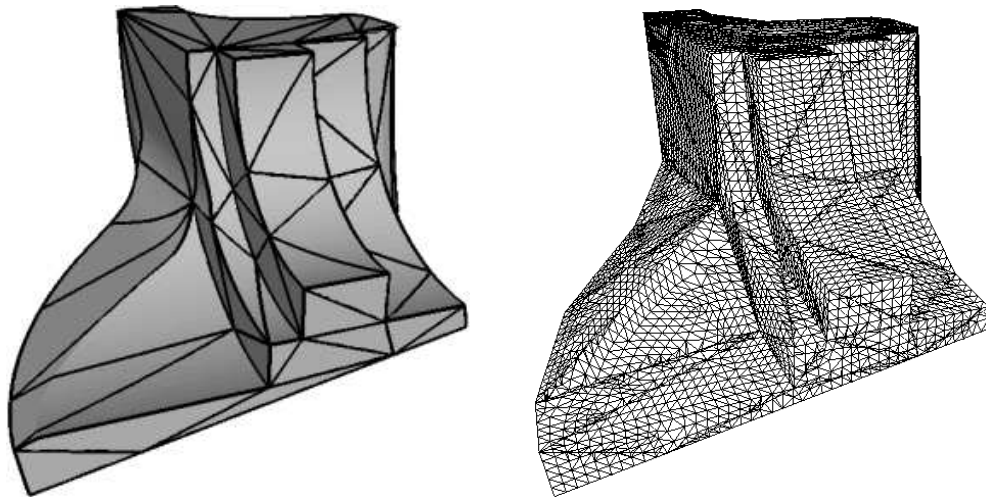


Fig. 7. Geodesic paths on $\Omega_{\mathcal{D}}$ (left) and parameterization of $\Omega_{\mathcal{T}}$ over $\Omega_{\mathcal{D}}$ (right).

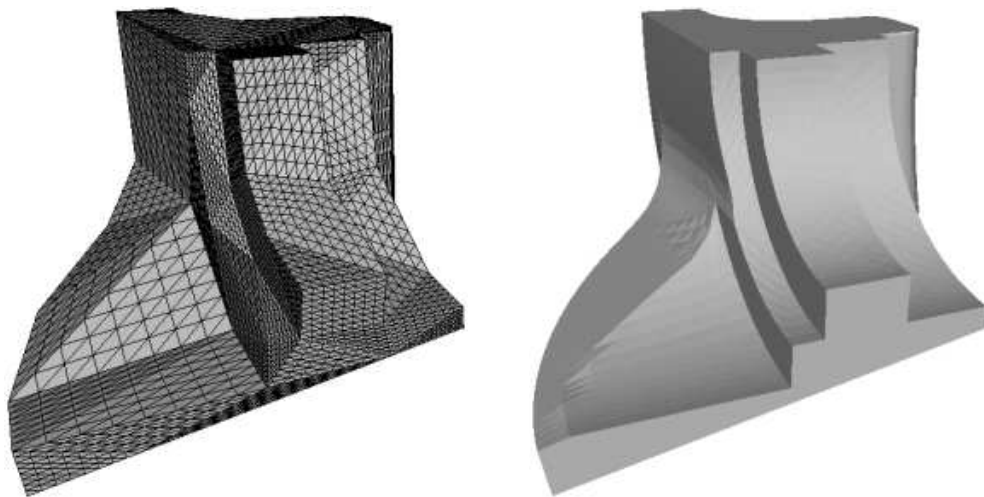


Fig. 8. Dyadic refinement \mathcal{D}^3 (left) and approximation $f^3(\Omega_{\mathcal{D}})$ of $\Omega_{\mathcal{T}}$ with 7,296 triangles (right).

For the 171 edges in \mathcal{D} we then computed the corresponding geodesic paths in $\Omega_{\mathcal{T}}$ as shown on the left of Fig. 7. These were then embedded into \mathcal{T} , yielding the refined triangulation \mathcal{T}' . Each triangular patch S_i of \mathcal{T}' was then parameterized over the corresponding triangle T_i of \mathcal{D} , the result being shown on the right of Fig. 7. Each linear system was solved using the bi-conjugate gradient method.

Figures 8 and 9 illustrate the use of the parameterization $\phi : \Omega_{\mathcal{D}} \rightarrow \Omega_{\mathcal{T}}$ for wavelet decomposition. First, we dyadically refined \mathcal{D} three times, yielding the triangulation \mathcal{D}^3 , and took $f^3 \in S^3$ to be the piecewise linear interpolant to ϕ . Its image $f^3(\Omega_{\mathcal{D}})$ approximates the given triangulation $\Omega_{\mathcal{T}}$; see Fig. 8. We then decomposed f^3 into $f^0 \in S^0$ and $g^i \in W^i$, $i = 0, 1, 2$. Sorting the 3,591 wavelet coefficients by magnitude and using only the largest 5% or 20%, respectively, to reconstruct f^3 gives the triangulations shown in Fig. 9.

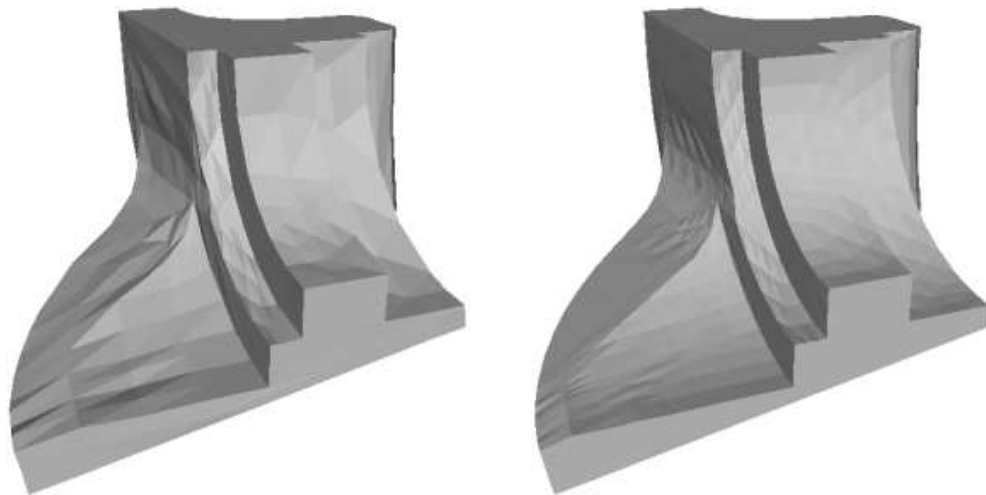


Fig. 9. Wavelet reconstruction of $f^3(\Omega_{\mathcal{D}})$ using 5% (left) and 20% (right) of the wavelet coefficients.

We have implemented the whole method in C++ and measured the following computation times on an SGI Octane with a 400 MHz R12000 processor.

mesh reduction	35 sec.
geodesic paths	44 sec.
parameterization	20 sec.
refinement	1 sec.
decomposition	2 sec.
reconstruction	1 sec.
total	103 sec.

Acknowledgments. This work was supported in part by the European Union research project “Multiresolution in Geometric Modeling (MINGLE)” under grant HPRN-CT-1999-00117.

References

1. Campagna, S., L. Kobbelt, and H.-P. Seidel, Efficient generation of hierarchical triangle meshes, in *The Mathematics of Surfaces VIII*, R. Cripps (ed.), Information Geometers, 1998, 105–123.
2. Chen, J. and Y. Han, Shortest paths on a polyhedron, *J. Comput. Geom. and Appl.* **6** (1996), 127–144.
3. Dijkstra, E. W., A note on two problems in connexion with graphs, *Numer. Math.* **1** (1959), 269–271.
4. Duchamp, T., A. Certain, T. DeRose, and W. Stuetzle, Hierarchical computation of PL harmonic embeddings, Technical Report, University of Washington, 1997.

5. Eck, M., T. DeRose, T. Duchamp, H. Hoppe, M. Lounsbery, and W. Stuetzle, Multiresolution analysis of arbitrary meshes, *Comp. Graphics (SIGGRAPH '95 Proc.)* **29** (1995), 173–182.
6. Floater, M. S., Parameterization and smooth approximation of surface triangulations, *Comput. Aided Geom. Design* **14** (1997), 231–250.
7. Floater, M. S., One-to-one piecewise linear mappings over triangulations, Preprint, University of Oslo, June 2001.
8. Floater, M. S. and E. G. Quak, Piecewise linear prewavelets on arbitrary triangulations, *Numer. Math.* **82** (1999), 221–252.
9. Floater, M. S., E. G. Quak, and M. Reimers, Filter bank algorithms for piecewise linear prewavelets on arbitrary triangulations, *J. Comput. Appl. Math.* **119** (2000), 185–207.
10. Gross, J. L. and T. W. Tucker, *Topological Graph Theory*, John Wiley & Sons, 1987.
11. Heckbert, P. S. and M. Garland, Survey of polygonal surface simplification algorithms, Technical Report, Carnegie Mellon University, 1997.
12. Kaneva, B. and J. O'Rourke, An implementation of Chen & Han's shortest paths algorithm, in *Proc. of the 12th Canadian Conf. on Comput. Geom.*, 2000, 139–146.
13. Kapoor, S., Efficient computation of geodesic shortest paths, in *ACM Symposium on Theory of Computing*, 1999, 770–779.
14. Kimmel R. and J. A. Sethian, Computing geodesic paths on manifolds, in *Proc. of National Academy of Sciences* **95**, 1998, 8431–8435.
15. Kobbelt, L., S. Campagna, and H.-P. Seidel, A general framework for mesh decimation, in *Graphics Interface 98 Proc.*, 1998, 43–50.
16. Lee, A., W. Sweldens, P. Schröder, L. Cowsar, and D. Dobkin, Multiresolution adaptive parametrization of surfaces. *Comp. Graphics (SIGGRAPH '98 Proc.)* **32** (1998), 95–104.
17. Mitchell, J. S. B., D. M. Mount, and C. H. Papadimitriou, The discrete geodesic problem, *SIAM J. Comput.* **16** (1987), 647–668.
18. Pham-Trong, V., N. Szafran, and L. Baird, Pseudo-geodesics on three-dimensional surfaces and pseudo-geodesic meshes, *Numer. Algorithms* **6** (2001), 305–315.
19. Pinkall, U. and K. Polthier, Computing discrete minimal surfaces and their conjugates, *Experimental Mathematics* **2** (1993), 15–36.
20. Polthier K. and M. Schmies, Straightest geodesics on polyhedral surfaces, in *Mathematical Visualisation*, C. Hege and K. Polthier (eds.), Springer, 1998, 135–150.
21. Praun E., W. Sweldens, and P. Schröder, Consistent mesh parameterizations, *Comp. Graphics (SIGGRAPH '01 Proc.)* (2001), 179–184.
22. Schröder, P. and W. Sweldens, Spherical wavelets: Efficiently representing functions on the sphere, *Comp. Graphics (SIGGRAPH '95 Proc.)* **29** (1995), 161–172.

Michael S. Floater
SINTEF
Post Box 124, Blindern
N-0314 Oslo, Norway
`mif@math.sintef.no`

Kai Hormann
Computer Graphics Group
University of Erlangen-Nürnberg
Am Weichselgarten 9
D-91058 Erlangen, Germany
`hormann@cs.fau.de`

Martin Reimers
Institutt for informatikk
Universitetet i Oslo
Post Box 1080, Blindern
N-0316 Oslo, Norway
`martinre@ifi.uio.no`